Submitted to Nuclear Instruments and Methods

UCRL-19952
Preprint

c. 2

IDENTIFICATION OF NUCLEAR FRAGMENTS BY A COMBINED TIME-OF-FLIGHT, ΔE-E TECHNIQUE

Gilbert W. Butler, A. M. Poskanzer, and D. A. Landis

August 1970

AEC Contract No. W-7405-eng-48

LAWRENCE RADIATION LABORATORY
UNIVERSITY of CALIFORNIA BERKELEY

UCRL-19952

DISCLAIMER

IDENTIFICATION OF NUCLEAR FRAGMENTS BY A COMBINED TIME-OF-FLIGHT, ΔE-E TECHNIQUE*

Gilbert W. Butler†, A. M. Poskanzer, and D. A. Landis

Lawrence Radiation Laboratory
Nuclear Chemistry Division
University of California
Berkeley, California 94720

August 1970

Abstract

Nuclear fragments of Z = 5 to 10 that resulted from the interaction of 5.5-GeV protons with uranium have been identified by a combined time-of-flight, ΔE-E technique. A thin ΔE detector was used so that the ΔE-E information provided only element resolution, not isotopic resolution. However, the measurement of the time-of-flight between the ΔE and E detectors together with the energy deposited in the E detector allowed the fragment mass to be determined. This technique enabled us to observe not only the major isotopes of these elements but also such neutron-rich nuclei as ^{18}C and ^{20}N. An improved algorithm for power-law particle identification is also described.

*Work performed under the auspices of the U. S. Atomic Energy Commission.

†Present Address: Chemistry Division, Argonne National Laboratory, Argonne, Illinois 60439.

Introduction

The unique determination of the atomic number Z and the mass number A of the products of a nuclear reaction is an essential part of the study of nuclear reactions. Identification of Z = 1 and 2 fragments is commonplace and there has been rapid progress recently in the development of on-line particle identification techniques for heavier fragments. In some cases this progress has been stimulated by the desire to establish the existence of extremely neutron-rich particle-stable light nuclei in order to provide further tests of the systematics of nuclear stability.

There are currently several methods of accomplishing the on-line identification of nuclear reaction products with Z of 5-10. To determine the mass of a nucleus, but not its charge, simple time-of-flight techniques have been used which allow measurements down to very low energies. Generally, one semiconductor detector is used for energy and time measurements with the other timing pulse coming from either an RF signal from a pulsed particle accelerator (see for example Ref. 1), or from a thin foil from which secondary electrons are collected with an electron lens. However, the most common technique that gives both nuclear charge and mass information is the use of a detector telescope consisting of a ΔE detector to measure the rate of energy loss of a particle and an E (stopping) detector to measure its residual energy.

With the ΔE-E technique there are three widely used methods for determining the identity of a particle from the information provided by the ΔE-E detector telescope. One method uses the relationship[2] $(E + \Delta E)\times(\Delta E) \propto AZ^2$, which is an approximation to the Bethe-Bloch formula for the rate of energy loss of a charged particle. Modified versions of this formula have been used to provide

isotopic resolution up through the oxygen region. The second widely used method of particle identification utilizing a ΔE-E detector telescope is based on the fact that the range-energy relationship of light nuclei can be approximated by the empirical power-law formula[3,4] $R = a\,\mathcal{E}^b$, where R is the range of a particle of energy $\mathcal{E}$, a is a constant that is characteristic of the particle, and the exponent b is approximately constant but is found to provide better isotopic resolution if it is allowed to decrease somewhat as Z increases. The exponent b is thus an adjustable parameter. For particles that obey this power-law relation the function $(E + \Delta E)^b - E^b$ can be shown to equal T/a, where T is the ΔE detector thickness. The quantity 1/a is approximately proportional to AZ^2. The third method involves storing a range-energy table for an isotope of interest in a computer[5]. Then from the ΔE-E information for each event the apparent thickness of the ΔE detector is calculated and a histogram is constructed. At the true thickness T of the detector there will be a peak for the isotope of interest, while other isotopes will peak at other apparent thicknesses. Other modifications of this method have been used[6]. All of these ΔE-E methods are limited by the energy resolution in the ΔE detector. Isotopic resolution becomes quite difficult with thin ΔE detectors for particles of $Z > 8$. A major limitation of the ΔE-E method is that for $Z > 5$ there is some overlap of the quantity AZ^2 for the heaviest isotopes of one element and the lightest isotopes of the next heavier element. This fact makes it difficult to establish unambiguously the identity of neutron-rich and neutron-deficient nuclei.

Another method of particle identification involves the addition of the fragment time-of-flight technique to the ΔE-E technique in order to provide an independent determination of the fragment masses. In these experiments[7-9] fragment flight times were determined between two ΔE detectors.

The mass number was calculated from the non-relativistic formula $A = \text{const.} \cdot \mathcal{E} \cdot t^2$, where t is the fragment flight time between the two ΔE detectors and $\mathcal{E}$ is the fragment energy during flight. Experiments utilizing this technique have had to rely heavily on the isotopic resolution obtained from the ΔE-E method because the time-of-flight mass resolution was slightly greater than one mass number. However, the technique was successful in establishing the identity of several neutron-rich light nuclei produced in the interaction of high-energy protons with heavy nuclei[7-9]).

Magnetic analysis together with an energy measurement by a semiconductor detector placed in the focal plane of a spectrometer has been used for heavy ion identification[10]). This method has some ambiguities because different isobars can have the same effective charge and also different nuclides can have similar values of Z_{eff}^2/A. The latter difficulty can be eliminated by the additional measurement of the time-of-flight of the ions[11]). Measurements have also been made by the combination of time-of-flight, energy, and magnetic quadrupole analysis[12]).

Another method of particle identification is the combination of the ΔE-E method with magnetic analysis[13]). A ΔE-E detector telescope was placed in the focal plane of a magnetic spectrometer to study heavy ion transfer reactions on a thorium target. This technique overcomes the usual difficulty of a magnetic analysis system by measuring the nuclear charge and not just the atomic charge. Isotopic resolution was obtained up through $Z = 10$ nuclei, and many new neutron-rich light nuclei were identified by this technique[14-16]).

In this paper we wish to report on improvements in particle identification techniques. First we discuss a new algorithm for particle identification by the power-law method. Secondly and more importantly we describe significant

improvements in the combined time-of-flight, ΔE-E technique. In the latter, modified electronic equipment was used to identify nuclear fragments of Z = 5-10 produced in the interaction of 5.5-GeV protons with uranium. Fragment flight times were determined between a ΔE and an E detector instead of between two ΔE detectors as in earlier experiments[7-9]). This made it possible to measure fragments that had lower energies and consequently longer flight times. The longer flight times greatly enhanced the time-of-flight determination and the lower energies meant greater fragment yields since the minimum energies measured were still above the peaks of the measured energy distributions for these high-energy reactions[17]). In this experiment the ΔE detector was thinner and provided only element resolution but the time-of-flight determination provided adequate mass resolution by itself.

Improved Algorithm for Power-Law Particle Identification

The power-law particle identifier was first developed at Berkeley by Goulding and Landis[3,4]). Details of the use of this type of particle identifier that employ either one or two ΔE detectors have been published elsewhere[18-20]). This method of particle identification does not give isotopic resolution for moderate energy nuclei with Z > 7 because of the inadequate energy resolution from the very thin ΔE detectors that are required. However, in an earlier experimental study of the interaction of high-energy protons with uranium[17]), we used a thin ΔE detector and were able to resolve elements (no isotopic resolution) from Be to Na, as shown by the particle spectrum in Fig. 1(a), which represents the output of the analog electronic system. The particle spectrum shown in Fig. 1(b) was calculated by an off-line computer from the ΔE and E data by the use of the power-law equation with a value of the exponent b of 1.40 to simulate the analog particle spectrum. A two-parameter contour plot

of the number of events versus particle signal and total energy for this same experiment is shown in Fig. 2(a). It can be seen from Fig. 2(a) that the particle signal is not independent of energy for a given element. For the lighter elements the decrease in particle signal with increasing energy could be corrected by raising the parameter b, but then the curvature at the lowest energies for the heavier elements would be considerably worse.

We have determined a modified power-law formula that is capable of automatically adjusting the exponent to obtain improved resolution for a broader spectrum of particles. It can be seen that the nuclei that deviate the most from the original power-law formula are the heavier elements with the lowest energies. Since these nuclei are the ones that have the highest dE/dx values, we decided to make the exponent decrease with the value of dE/dx given by the energy deposited in the ΔE detector. The modified algorithm has the following form:

$$\left[\left(\frac{E + \Delta E}{k}\right)^n - \left(\frac{E}{k}\right)^n\right]^{1/2} ,$$

where the exponent is $n = b - \frac{c\,\Delta E}{T}$. We have taken the units of c to be mg/cm^2-MeV. In this formula the two energy terms are divided by a large constant (we use k = 300 but the exact value is not critical). This is done because with a variable exponent it is necessary to normalize the spectra at a high energy where the exponent is approximately constant. The square root of the particle signal is used simply because it makes the signal proportional to Z instead of to Z^2. It should be mentioned that in the search for the best b and c values to use in this equation we have relied on range-energy and energy-loss programs written at this laboratory[21,22].

The dramatic improvement in particle spectrum resolution that results from the use of the modified power-law equation with the appropriate b and c

parameters, is illustrated in Figs. 1(c) and 2(b), which represent the same data reprocessed according to this modified equation. (The calculations to process each event took about 300 μsec on a Control Data Corporation 6600 computer.) The modified equation produces the desired effect of making the particle signal more independent of energy and the resolution is improved to such an extent that the isotopes ^{7}Be and ^{8}B are clearly resolved in Fig. 1(c). (^{8}Be and ^{9}B do not appear in the spectra because their half lives are too short to allow them to reach the detector.) The widths of the other peaks are mainly due to the high yields of the many unresolved isotopes of each element[17]). We have shown that it is possible to obtain element resolution up to argon (Z = 18) with a 20-μm ΔE detector[17]) and this method could probably be extended to even heavier elements with the use of thinner ΔE detectors.

Experimental——Combined Time-of-Flight, ΔE-E Technique

The experiment was performed by using the 5.5-GeV external proton beam of the Bevatron to bombard a uranium metal target of 27 mg/cm^2 thickness. Beam pulses 0.8 sec long and containing an average of 10^{12} protons occurred every six seconds. Many of the details of the experimental equipment that do not involve time-of-flight have been published elsewhere[17]) and they will not be discussed here unless there are significant differences.

A detector telescope consisting of three phosphorus-diffused silicon detectors was placed at 90° to the beam to view the fragments emitted from the target. The 22-μm ΔE detector was 14.5 cm from the center of the target, and the 112-μm E detector was 25.7 cm further away with a rejection detector right behind it. The ΔE and E detectors had sensitive areas of 5 × 7 mm and were collimated to 4 × 6 mm by copper collimators 0.8 mm thick.

The electronic circuitry that was used for this combined time-of-flight, particle identification experiment is schematically illustrated in Fig. 3. Fast rise-time linear preamplifiers were integrally mounted with the ΔE and E detectors in the vacuum chamber as shown in Fig. 4. The detector was DC connected to the input FET by the shortest possible path to minimize electronic ringing due to inductance in the input circuit. Signal feedback around the front end of the preamplifier was also avoided because of its tendency to produce ringing on signals. The voltage produced across the fixed detector capacitance was amplified by a high-transconductance (50 mA/V) FET, whose operating conditions were stabilized by DC (low frequency) feedback to prevent changes in the operating point caused by leakage current changes in the detector due to radiation damage.

A block diagram of the preamplifier, fast amplifier and discriminator system is shown in Fig. 5. The electronic rise time of the preamplifier was less than one nsec, and its decay time constant was about 60 μsec in the case of the ΔE channel and somewhat less for the E channel because of the lower detector capacitance. Signals from the preamplifiers were sent through wide-band low-loss 50-Ω coaxial cables to the fast amplifiers in the counting area. The amplifiers clipped the signals to 10 nsec and supplied them to zero-crossing discriminators. The rise time of the signals from the fast amplifiers was 2.5 nsec and the change in rise time up to a maximum output of ± 2 V caused less than 100 psec change in the crossover point of the double-clipped signal developed in the crossover discriminator. The zero-crossing discriminator was a modified version of one developed for use with fast photo-tubes[23]). It has a dynamic range of over 100 to 1 with a maximum input of 2 V. The signal at the positive input triggered the pedestal circuit whose output current was set just to trigger the tunnel diode discriminator. When the signal coming into the negative input and

the pedestal signal were added the tunnel diode discriminator triggered at the zero-crossing point of the double-delay-line clipped signal.

The time walk in the discriminator output as a function of input signal size and the FWHM timing spread of the fast system was measured with a fast pulse generator giving the results shown in Table I. For the measurements given in Table I(A), the timing of the ΔE system with reference to the input signal was determined (a 220 pF capacitor was used to simulate the detector). These measurements were accomplished by starting a time-to-amplitude converter (TAC) with the pulser and stopping it with the ΔE discriminator output signal. For the measurements in Table I(B) and I(C), the detectors were connected and the time difference between the ΔE and E discriminator outputs was measured. For Table I(B), the pulser supplied a fixed signal equivalent to 50 MeV to the E preamplifier while the ΔE signal was varied from 5 to 50 MeV. In Table I(C) the ΔE signal was fixed at 50 MeV and the E signal was varied.

During the actual experiment the fast discriminator outputs were sent to a TAC that operated in the 0-100 nsec range. The TAC was started by the E discriminator signal and stopped by the signal from the ΔE discriminator delayed by 50 nsec. The time spectrum was thereby inverted so the flight time of a fragment was $(t_0 - t_{TAC})$, where t_0 was a zero-time reference whose value it was necessary to determine. The system was set up to measure flight times ranging from 10 to 30 nsec--adequate to cover the flight times of all fragments from B to Ne in the energy range 10 to 40 MeV over a 25.7 cm flight path.

The ΔE, E, TAC and particle signals for each valid event were digitized and sent to a small on-line computer and were then stored on magnetic tape. The details of this computer system have been published elsewhere[17]). The computer

performed an on-line mass calculation by computing the quantity $E(t_0 - t_{TAC})^2$ which is proportional to Et^2 (and thus to mass) for the correct value of t_0. This on-line calculation and the associated oscilloscope display were of considerable use for monitoring purposes during the long experiments but the final data reduction was done with a CDC-6600 computer, where a Fortran program used the raw data tape to calculate a mass spectrum corrected for the walk of the timing signals with pulse height. This program also calculated a particle spectrum from the modified power-law equation described earlier.

A preliminary experiment was done with the ΔE and E detectors 3.2 cm apart to set up the electronic equipment and to determine an approximate value of t_0 to be used in the on-line mass calculation. During this experiment it was found that the collection time characteristics of the E detector had a marked effect on the fast timing resolution. Some improvement in resolution was obtained when the E detector bias was raised from 100 V to 200 V so the latter value was used throughout the experiment. Also, in order to obtain the best time resolution, the E detector was positioned so that the negatively-biased side faced the target. This configuration provided the shortest path for the holes (which are only one-third as mobile as electrons in silicon at room temperature) since most of the fragments of interest penetrated only a short distance into the E detector. The timing resolution and walk measurements were made by collecting the TAC spectra for all the fragments that deposited from 18-20 MeV in the E detector. The TAC spectra were sorted on the analog particle signal (which was sufficient to provide element resolution) and then corrected for the appropriate flight times over the short flight path. The results of these measurements are shown in Table II. The resolutions have been corrected

for the spread in velocities due to the 2 MeV wide window placed on the E signal. The listed ΔE energies were calculated from range-energy tables for the highest yield isotope of each element (ie., ^{11}B, ^{13}C, etc.). It can be seen that the walk and resolution are not as good as with the pulser. This is probably due mainly to the collection time in the E counter, which is a function of the range of the particles. An improvement could be made by using a somewhat thinner E counter at still higher bias or by cooling the detector to a low temperature.

Results——Fragments from Uranium + 5.5-GeV Protons

The particle spectrum obtained during a 57 hr experiment is shown in Fig. 6. This spectrum was calculated from the improved power-law equation with the parameters b = 1.84 and c = 0.064. We believe the resolution is not as good as that in Fig. 1(c) because of a greater non-uniformity of the ΔE detector used in this experiment. However, the resolution obtained was adequate for the determination of the nuclear charge of the fragments.

The technique that was used for determining the corrections to the time-of-flight data that were needed to compensate for the walk of the timing signals with pulse height in both of the detectors will be described in some detail since it was a very crucial part of the final data analysis. The crude t_0 values determined in the short flight path experiment were not adequate and thus the final data were used for this purpose. First the raw data tape was processed off-line several times using different values of t_0 to calculate the mass spectrum for those events that deposited from 18-20 MeV in the E detector. This processing was done by sorting the TAC signal on the analog particle signal, which was sufficient to provide element separation, and calculating the

mass spectra in order to determine the value of t_0 that gave the best mass resolution for each element. This procedure effectively determined the timing walk due to the variation of the ΔE pulse height, which varied from about 11.5 MeV for a boron fragment to 34 MeV for a fluorine fragment. The walk of the timing signal with pulse height in the E detector was determined in a similar manner by processing those events that deposited 10-12 MeV and also 36-40 MeV in the E detector. However, now the value of t_0 for each element was chosen to put the isotopes of that element in the same mass channels as did the best value of t_0 obtained from the 18-20 MeV data. The resultant array of t_0 values was fitted by a linear least squares program to an equation that contained terms linear in ΔE and E and a term with the product (ΔE)×(E). This t_0 equation was then used during the final data reduction at the CDC-6600 computer to determine the walk-corrected value of t_0 for each event.

The corrected mass spectrum containing all of the fragments that deposited from 15 to 30 MeV in the E detector is shown in Fig. 7. Each mass peak in this spectrum contains some contribution from more than one isobar. The mass resolution (FWHM) is 4.0% at mass 11 and 4.1% at mass 18. The time resolution of the pulser was 140 psec. The time resolution for the particles was about 250 psec. This was calculated from the measured mass resolution, with a correction for the contribution from the energy resolution.

A two-parameter contour plot of the number of events versus particle signal and mass signal is shown in Fig. 8. The element lines increase with mass simply because the particle signal is somewhat a function of the mass of the isotope as well as its charge. With the walk corrections that we used the mass number lines are not all vertical, which means that the mass resolution was somewhat better than is indicated in Fig. 7. It is clear from this contour plot

that the charge and mass resolution was sufficiently good to separate not only the major isotopes of the elements boron to neon, but also many of the neutron-rich nuclides. This is illustrated more clearly in Fig. 9, which is the carbon mass spectrum obtained by projecting the carbon data in Fig. 8 onto the mass axis. In this experiment ^{17}C was produced in much greater yield than in our earlier experiment[7]). Even ^{18}C is easily distinguishable in Fig. 9, and we thus confirm recent experiments[14]) concerning the particle stability of this nuclide. Unfortunately, background problems prevent us from being able to say anything about the particle stability of nuclides of carbon heavier than ^{18}C, such as ^{19}C, which has been reported recently as being particle stable[9]). Also, as seen in Fig. 8, our data clearly confirm the recent work[14,15]) in which the particle stability of the neutron-rich nuclei ^{20}N, ^{22}O, ^{23}F, and ^{25}Ne was established by observing these nuclei during a study of heavy ion transfer reactions on a heavy nucleus.

Our experimental system does have some residual background problems, as can be seen in Figs. 8 and 9, especially in the low mass regions. We think that most of the background was primarily caused by events in which the time-of-flight signal of a real event was distorted by a chance coincidence with a light fragment, such as a lithium isotope, that registered in the E detector but did not deposit enough energy in the ΔE detector to trigger it. The number of chance coincidence events could be reduced by using a very fast pile-up rejector to trigger down to very small ΔE signals. However, this might be difficult because the counting rate in the ΔE detector at low energies was over 10^5 sec^{-1} during this experiment.

Discussion

The combined ΔE-E, time-of-flight method of particle identification described here is potentially capable of identifying individual nuclei with moderate energies up to much higher mass and charge than is possible with the ΔE-E method by itself. This is illustrated more clearly in Fig. 10, which is a graphical summary of the limitations of the ΔE-E method of particle identification. The solid lines represent the minimum total energy that is necessary to observe a nuclide with a certain thickness of ΔE detector. These total energies include both the minimum energies in the E detector that are listed near the bottom of the graph and the energies needed to penetrate the ΔE detector. The approximate limits of isotopic resolution by the ΔE-E technique are represented by the dashed line. That is, to the left of the dashed line individual isotopes can be resolved, but to the right of the line only element separation can be obtained. The use of the ΔE-E method for determining nuclear charge only should be very useful for elements even with Z > 18 (argon).

The use of the time-of-flight technique to determine the masses of various nuclear reaction products has become more widespread in recent years. The limitation of this technique is shown in Fig. 11. This is a graph of the energy at which adjacent masses are just resolvable as a function of the mass number of the nuclide. We have defined just resolvable as that resolution which gives a two to one peak-to-valley ratio for equal height gaussian distributions. For adjacent mass peaks this corresponds to a FWHM of $\sqrt{2}/2$ mass numbers or to a σ of 0.30 mass numbers. These curves were calculated from the following formula, which assumes that the energy resolution is small compared to the time resolution:

$$\mathcal{E} = \frac{0.129\ (\Delta A)^2 (d)^2}{A\ (\Delta t)^2} \quad ,$$

where $\mathcal{E}$ is the fragment energy in MeV, A is the mass number, ΔA is the mass

resolution, d is the flight path in cm, and Δt is the time resolution in nsec. Where the lines curve they were calculated with relativistic equations which were solved parametrically as a function of velocity. The important quantity in Fig. 11 is the ratio of the flight path to the time resolution, $d/\Delta t$, and each of the curves is labeled by this quantity in cm/nsec. It is clear from the steepness of these curves that one must have either a long flight path or very good time resolution to be able to resolve masses in the medium and high mass regions. However, the technique described here has the additional advantage that the flight times are measured after the fragments penetrate the ΔE detector and therefore they have lower energies and longer flight times. A difficulty in applying this technique to absolute cross section measurements would be the evaluation of the correction for loss from multiple scattering.

Acknowledgments

We would like to express our appreciation to F. S. Goulding for his excellent advice during the development of the fast electronics and to E. K. Hyde for his support and interest throughout the experiment. We also acknowledge R. P. Lothrop, M. D. Roach, and W. L. Searles for providing the detectors and for constructing some of the electronics, and the Bevatron staff for their cooperation.

References

1. C. N. Davids, H. Laumer and S. M. Austin, Phys. Rev. C 1 (1970) 270.

2. M. W. Sachs, C. Chasman and D. A. Bromley, Nucl. Instr. Methods 41 (1966) 213.

3. F. S. Goulding, D. A. Landis, J. Cerny and R. H. Pehl, Nucl. Instr. Methods 31 (1964) 1.

4. F. S. Goulding, D. A. Landis, J. Cerny and R. H. Pehl, IEEE Trans. Nucl. Sci. 13, no. 3 (1966) 514.

5. B. Hird and R. W. Ollerhead, Nucl. Instr. Methods 71 (1969) 231.

6. C. Brun, J. Galin, B. Gatty, M. Lefort and X. Tarrago, Rev. Phys. Appl. 4 (1969) 107.

7. A. M. Poskanzer, G. W. Butler, E. K. Hyde, J. Cerny, D. A. Landis and F. S. Goulding, Phys. Letters 27B (1968) 414.

8. T. D. Thomas, G. M. Raisbeck, P. Boerstling, G. T. Garvey and R. P. Lynch, Phys. Letters 27B (1968) 504.

9. G. M. Raisbeck, P. Boerstling, P. Riesenfeldt, T. D. Thomas, R. Klapisch and G. T. Garvey, Phys. Letters, to be published.

10. J. C. Jacmart, M. Liu, F. Mazloum, M. Riou, J. C. Roynette and C. Stephan, Rev. Phys. Appl. 4 (1969) 99.

11. M. Lefort, J. C. Jacmart, J. Peter, M. Riou, J. C. Roynette, C. Stephan and X. Tarrago, in Nuclear Reactions Induced by Heavy Ions, ed. R. Bock and W. R. Hering (North-Holland Publishing Co., Amsterdam, 1970), p. 795.

12. A. A. Vorob'ev, V. T. Gratchev, A. P. Komar, I. A. Kondurov, A. M. Nikitin and D. M. Seliverstov, Soviet Atomic Energy 27 (1969) 713.

13. A. G. Artukh, V. V. Avdeichikov, J. Erő, G. F. Gridnev, V. L. Mikheev and V. V. Volkov, Nucl. Instr. Methods 83 (1970) 72.

14. A. G. Artukh, G. F. Gridnev, V. L. Mikheev and V. V. Volkov, Nucl. Phys. A137 (1969) 348.

15. A. G. Artukh, V. V. Avdeichikov, G. F. Gridnev, V. L. Mikheev, V. V. Volkov and J. Wilczynski, Phys. Letters 31B (1970) 129.

16. A. G. Artukh, V. V. Avdeichikov, L. P. Chelnokov, G. F. Gridnev, V. L. Mikheev, V. I. Vakatov, V. V. Volkov and J. Wilczynski, Phys. Letters 32B (1970) 43.

17. A. M. Poskanzer, G. W. Butler and E. K. Hyde, Phys. Rev. C, to be published.

18. J. Cerny, S. W. Cosper, G. W. Butler, H. Brunnader, R. L. McGrath and F. S. Goulding, Nucl. Instr. Methods 45 (1966) 337.

19. A. M. Poskanzer, S. W. Cosper, E. K. Hyde and J. Cerny, Phys. Rev. Letters 17 (1966) 1271.

20. G. W. Butler, J. Cerny, S. W. Cosper and R. L. McGrath, Phys. Rev. 166 (1968) 1096.

21. C. C. Maples, Jr. and J. Cerny, personal communication.

22. P. G. Steward, Lawrence Radiation Laboratory Report UCRL-18127 (1968) unpublished.

23. D. L. Wieber and H. W. Lefevre, IEEE Trans. Nucl. Sci. 13, no. 1 (1966) 406.

Table I. Walk and resolution of the fast electronics as measured with a pulse generator.

			Energy (MeV)			
			5	10	20	50
A.	ΔE system only, with 220 pF capacitor	walk(psec)	+10	+20	+20	0
		FWHM(psec)	90	55	35	20
B.	Relative time E → ΔE (E fixed at 50 MeV), detectors connected	walk(psec)	+60	+20	-25	0
		FWHM(psec)	250	120	70	50
C.	Relative time E → ΔE (ΔE fixed at 50 MeV), detectors connected	walk(psec)	-10	+20	+5	0
		FWHM(psec)	120	70	70	50

Table II. Walk and resolution obtained in a short flight-path experiment.

Fragment	ΔE (MeV)	E (MeV)	walk (psec)	FWHM (psec)
B	11.5	19	+86	260
C	16.8	19	+22	260
N	21.9	19	-71	260
O	28.1	19	-72	260
F	34.2	19	0	260
Pulser				85

Figure Captions

Fig. 1. Particle spectra resulting from the interaction of 5.5-GeV protons with a uranium target. The detector telescope consisted of a 20-μm ΔE detector and a 300-μm E detector. All three spectra are from the same experiment but the data were processed in different ways, as discussed in the text. The pulser peak is split in (b) and (c) because the least significant bit of the ADC was not functioning during the experiment. The Li data were removed from the figure.

Fig. 2. Contour plots of particle signal and total energy corresponding to the data of Fig. 1(b) and 1(c). The contour levels are at 10, 20, 50, 100, 200, 500, 1000, 2000 and 5000 events. The array size was 64 × 32 and accounts for the coarseness of the plots.

Fig. 3. Schematic diagram of the electronics.

Fig. 4. Photograph of the E detector and preamplifier. The detector, on the circular wafer, is 5 × 7 mm.

Fig. 5. Block diagram of the fast electronics for the time-of-flight measurements.

Fig. 6. Particle spectrum obtained in this experiment. The data shown in Figs. 6-9 represent only those valid events that deposited from 15 to 30 MeV in the E detector.

Fig. 7. Mass spectrum of Z = 5 to 11 fragments obtained in this experiment.

Fig. 8. Contour plot of mass signal and particle signal for this experiment. The contour levels are at 5, 10, 20, 50, 100, 200, 500, 1000, 2000, 5000, 10,000 and 20,000 events. The dimensions of the array are 128 × 64. The elements and mass numbers are indicated.

Fig. 9. Mass spectrum of carbon isotopes that was obtained by projecting the carbon data in Fig. 8 onto the mass axis.

Fig. 10. Graph showing the limits of the ΔE-E method of particle identification. Plotted is the minimum total energy needed to penetrate the indicated ΔE detector thickness and leave the minimum energy in the E detector shown at the bottom of the figure. The dashed line indicates the approximate limits of isotopic resolution. To the right of this line only element resolution is obtained.

Fig. 11. Graph for time-of-flight experiments showing the energy during flight at which adjacent isotopes are just resolvable. The curves are labeled by the ratio of the flight path $\underline{d}$ (in cm) to the time resolution Δt (in nsec).

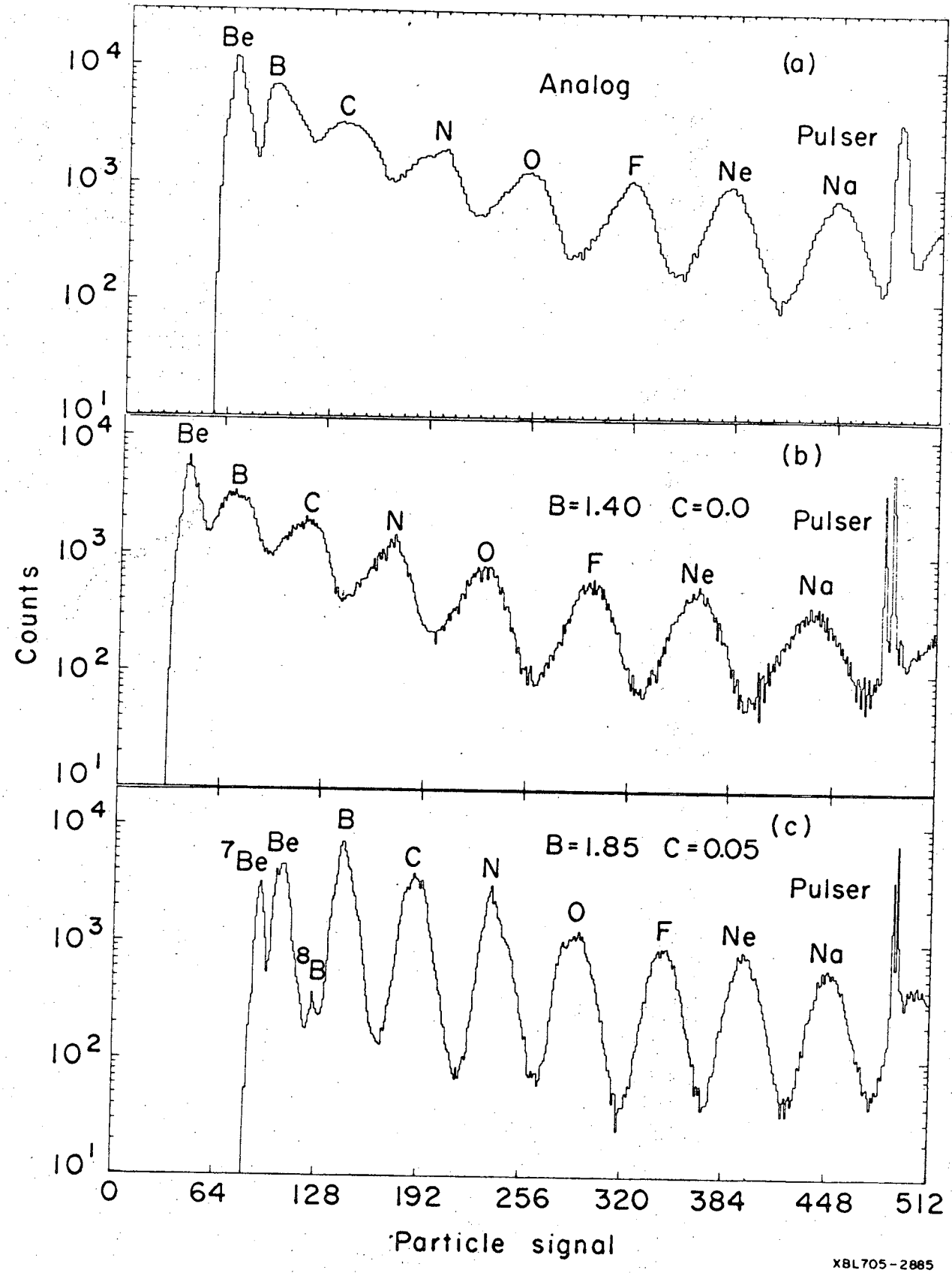
Be
B
C
N
O
F
Ne
Na
Analog
Pulser
(a)
(b)
B=1.40 C=0.0
(c)
B=1.85 C=0.05
^{7}Be
^{8}B
Counts
Particle signal
XBL705-2885

Fig. 1

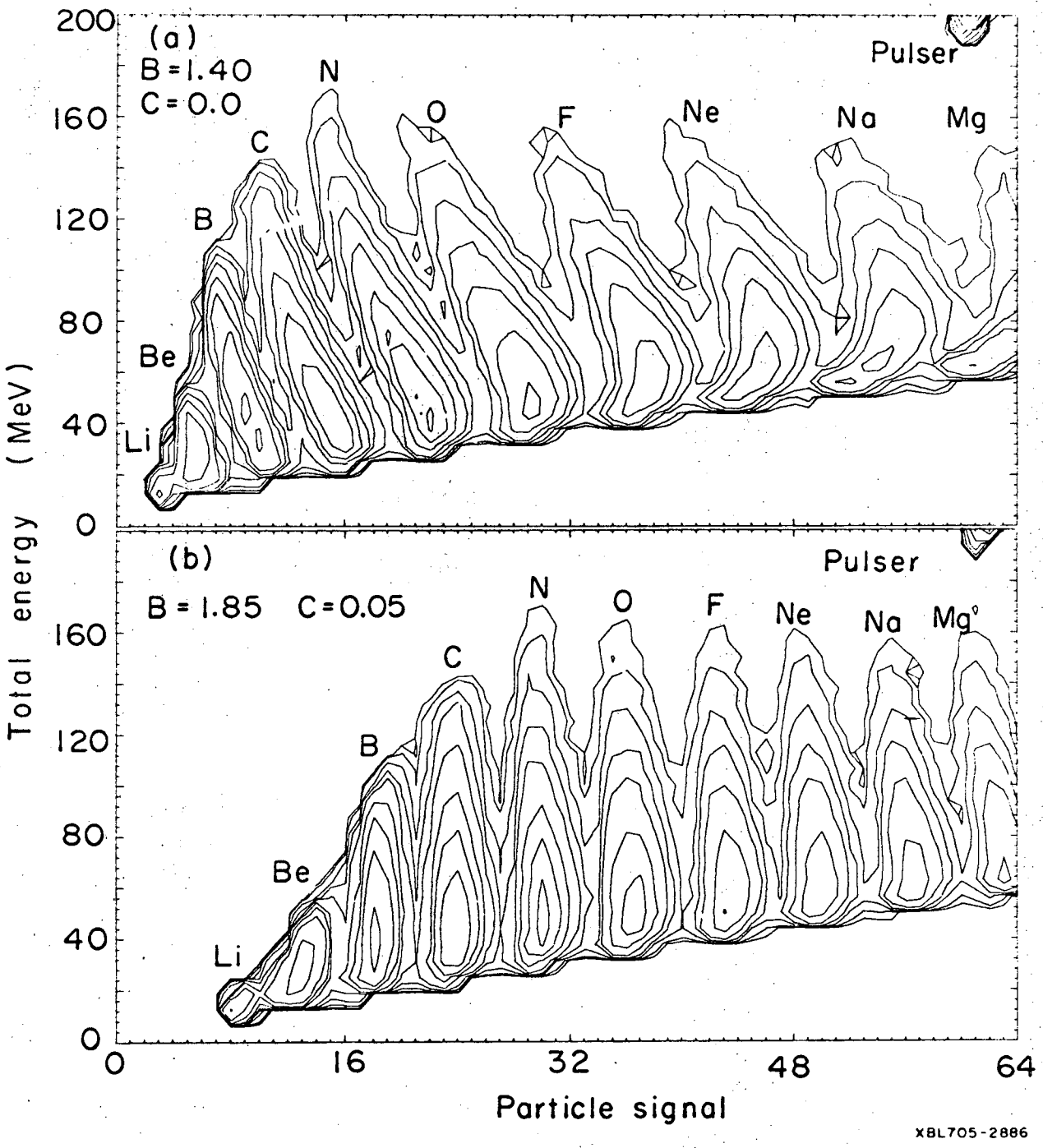
(a)
B = 1.40
C = 0.0
Pulser
Li
Be
B
C
N
O
F
Ne
Na
Mg
(b)
B = 1.85 C = 0.05
Pulser
Li
Be
B
C
N
O
F
Ne
Na
Mg
Total energy (MeV)
Particle signal
0
40
80
120
160
200
16
32
48
64
XBL705-2886

Fig. 2

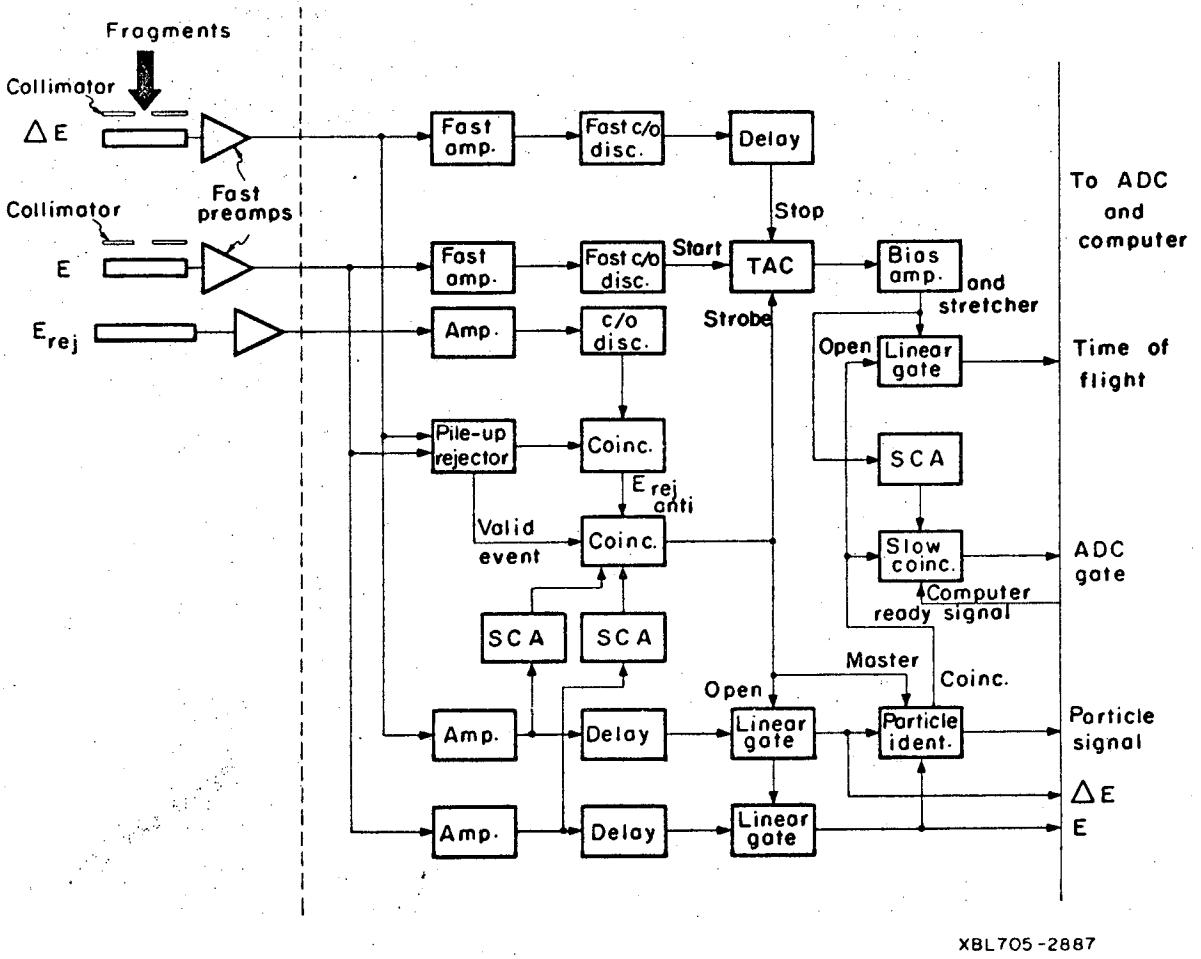

XBL705-2887

Fig. 3

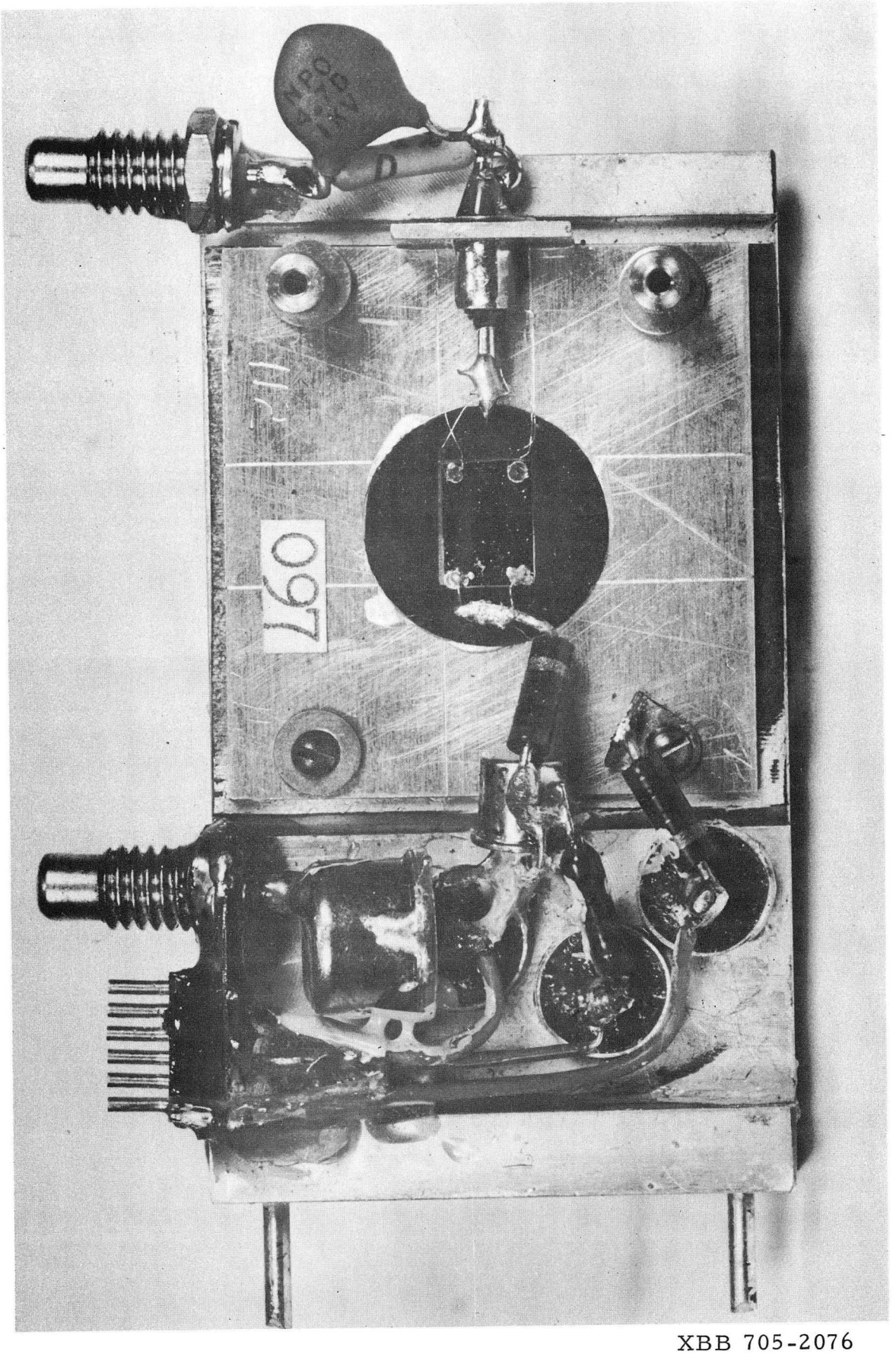

XBB 705-2076

Fig. 4

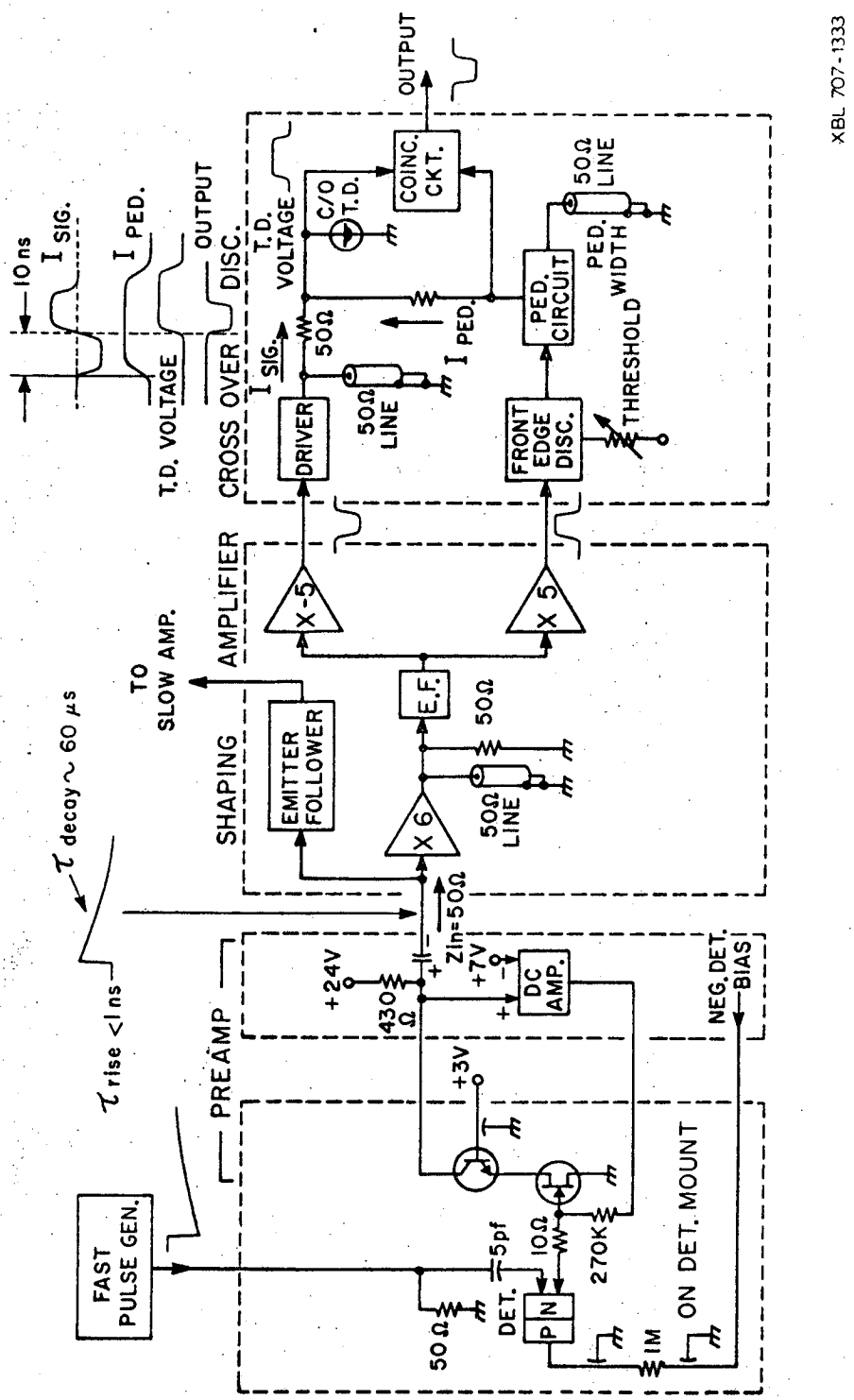
FAST PULSE GEN.
PREAMP
ON DET. MOUNT
NEG. DET. BIAS
DC AMP.
+24V
+7V
+3V
430 Ω
Zin=50Ω
5pf
10Ω
270K
50 Ω
DET.
P
N
1M
τ rise <1 ns
τ decay ~ 60 μs
SHAPING
EMITTER FOLLOWER
E.F.
X 6
50Ω LINE
TO SLOW AMP.
AMPLIFIER
X -5
X 5
CROSS OVER
DISC.
T.D. VOLTAGE
OUTPUT
I SIG.
I PED.
10 ns
DRIVER
C/O T.D.
COINC. CKT.
FRONT EDGE DISC.
PED. CIRCUIT
THRESHOLD
PED. WIDTH
XBL 707-1333

Fig. 5

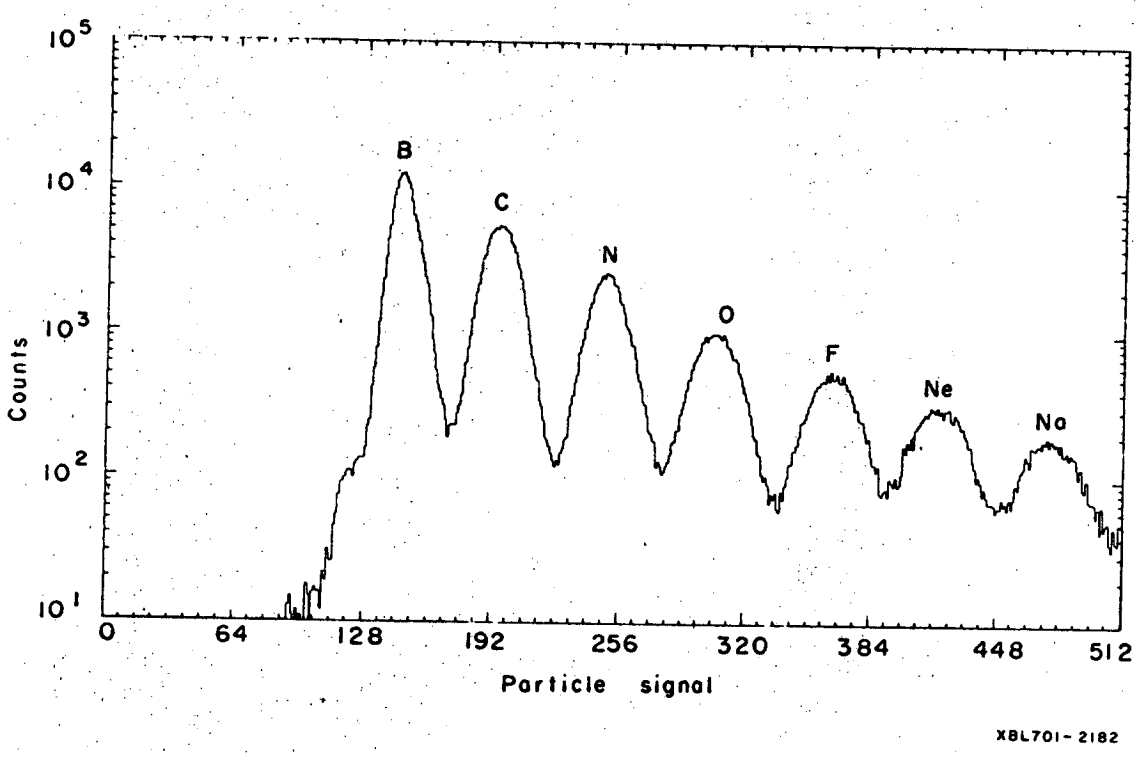
10^5
10^4
10^3
10^2
10^1
Counts
B
C
N
O
F
Ne
Na
0
64
128
192
256
320
384
448
512
Particle signal
XBL701-2182

Fig. 6

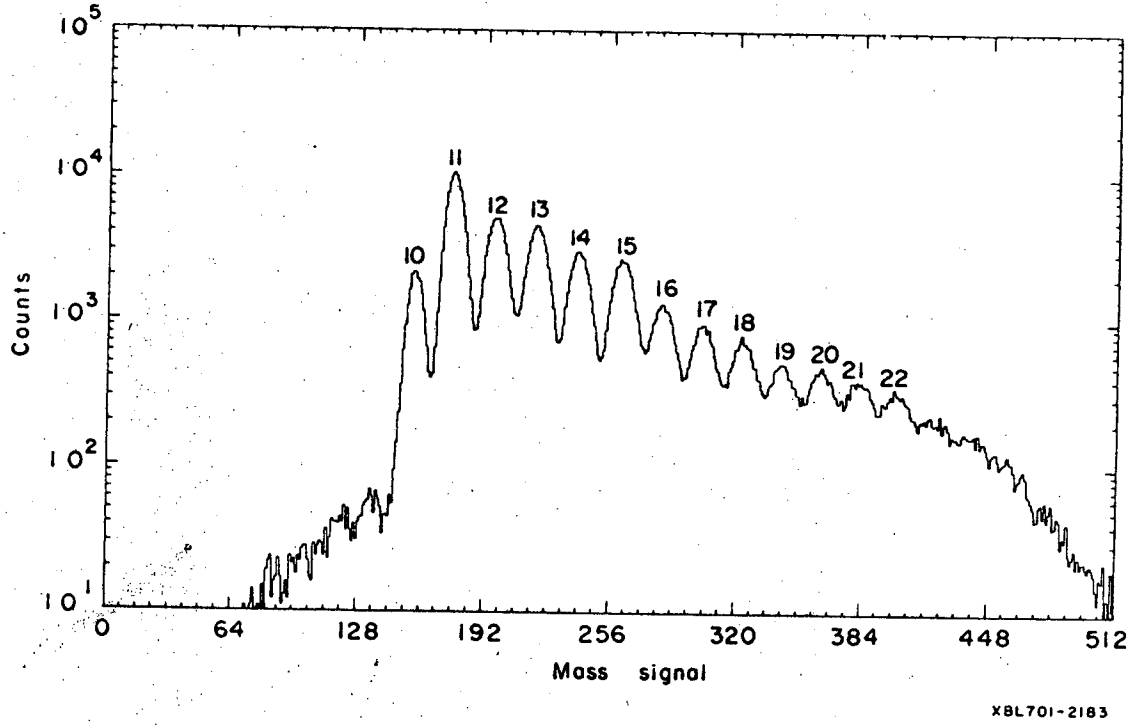
Counts
10^5
10^4
10^3
10^2
10^1
0
64
128
192
256
320
384
448
512
Mass signal
10
11
12
13
14
15
16
17
18
19
20
21
22
XBL701-2183

Fig. 7

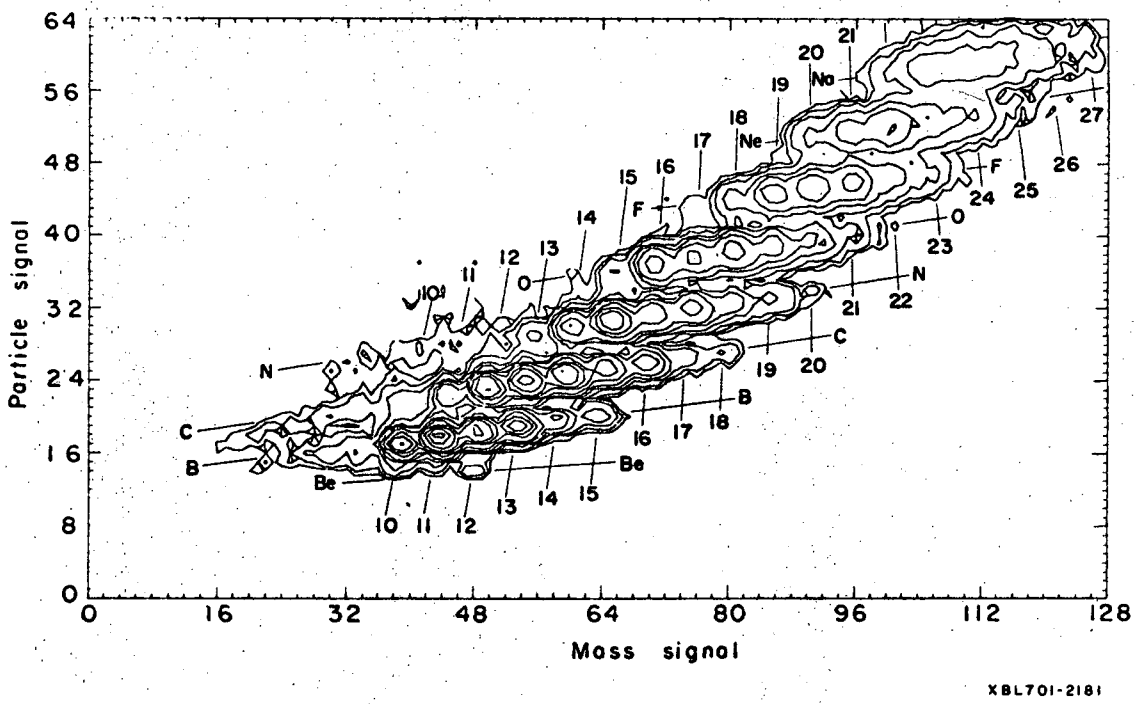
Particle signal
Mass signal
0
8
16
24
32
40
48
56
64
0
16
32
48
64
80
96
112
128
XBL701-2181

Fig. 8

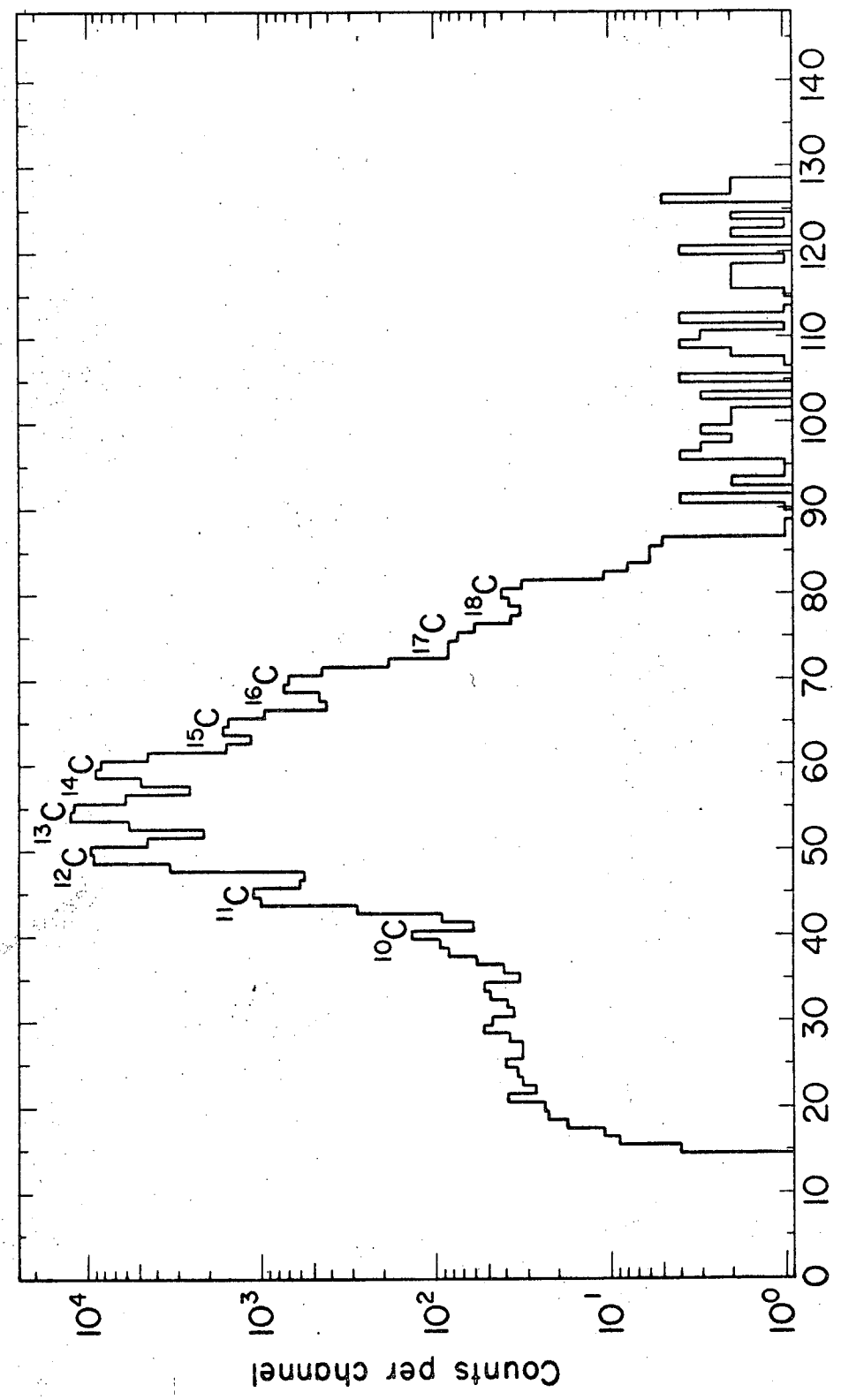

XBL705-2833

Fig. 9

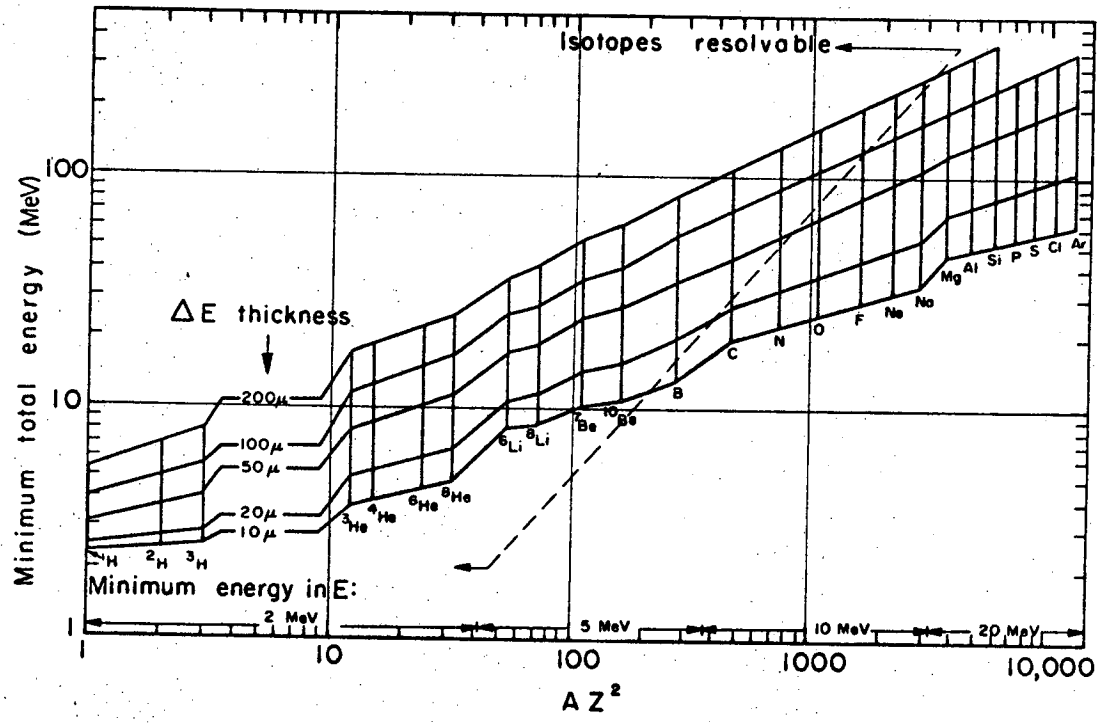
Isotopes resolvable
ΔE thickness
200μ
100μ
50μ
20μ
10μ
Minimum total energy (MeV)
100
10
1
Minimum energy in E:
2 MeV
5 MeV
10 MeV
20 MeV
1
10
100
1000
10,000
AZ²
XBL697-3342

Fig. 10

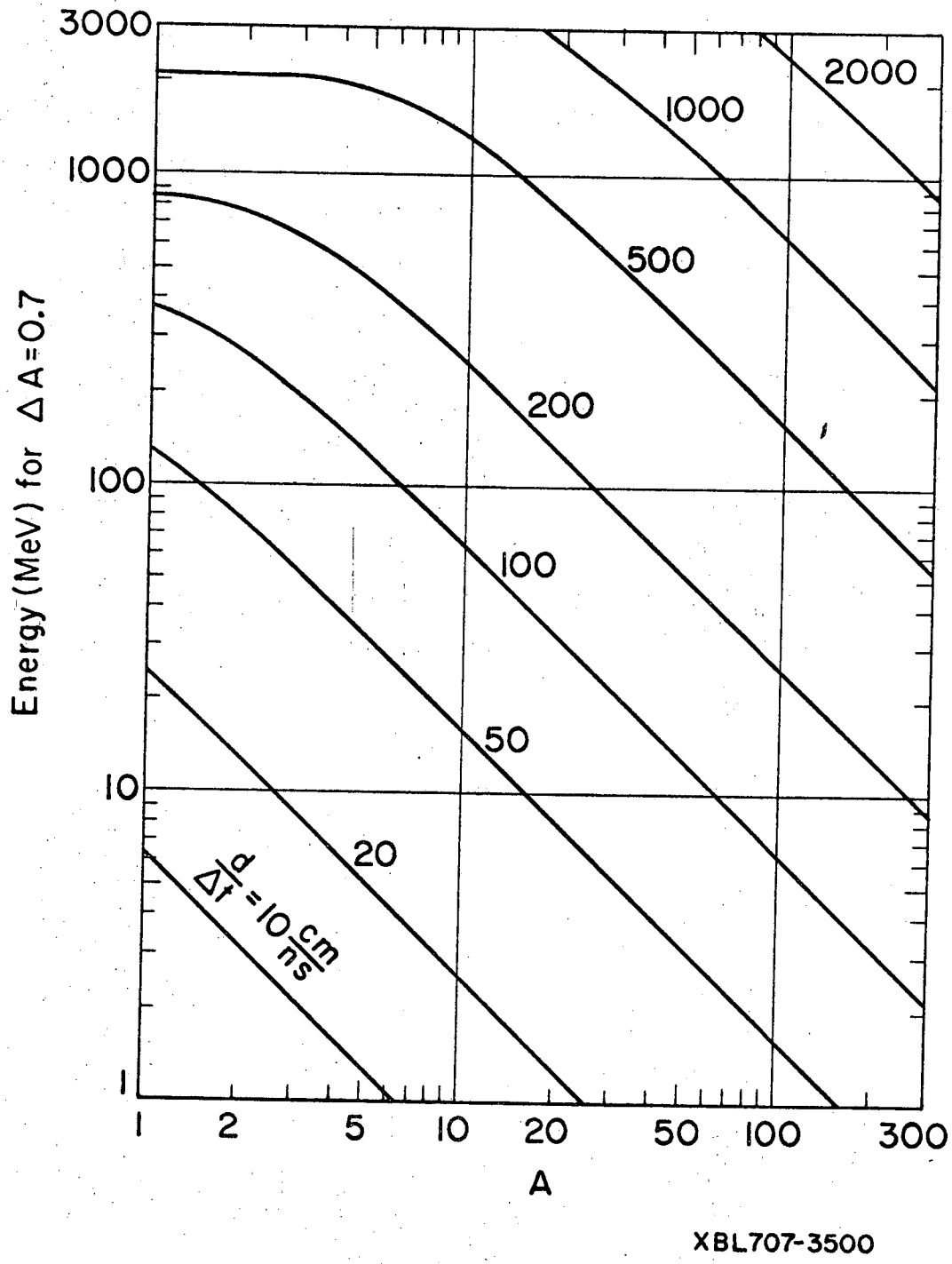
3000
1000
100
10
1
Energy (MeV) for ΔA=0.7
2000
1000
500
200
100
50
20
d/Δt = 10 cm/ns
1
2
5
10
20
50
100
300
A
XBL707-3500

Fig. 11

LEGAL NOTICE

TECHNICAL INFORMATION DIVISION
LAWRENCE RADIATION LABORATORY
UNIVERSITY OF CALIFORNIA
BERKELEY, CALIFORNIA 94720